Computed tomography-based prediction of pancreatitis following biliary metal stent placement with the convolutional neural network

OPEN ACCESS

Authors
Tsuyoshi Hamada[1,2], Koichiro Yasaka[3], Yousuke Nakai[1,4], Rintaro Fukuda[1], Ryunosuke Hakuta[1], Kazunaga Ishigaki[1], Sachiko Kanai[1], Kensaku Noguchi[1], Hiroki Oyama[1], Tomotaka Saito[1], Tatsuya Sato[1], Tatsunori Suzuki[1], Naminatsu Takahara[1], Hiroyuki Isayama[5], Osamu Abe[3], Mitsuhiro Fujishiro[1]

Institutions
1 Department of Gastroenterology, Graduate School of Medicine, The University of Tokyo, Tokyo, Japan
2 Department of Hepato-Biliary-Pancreatic Medicine, Cancer Institute Hospital, Japanese Foundation for Cancer Research, Tokyo, Japan
3 Department of Radiology, Graduate School of Medicine, The University of Tokyo, Tokyo, Japan
4 Department of Endoscopy and Endoscopic Surgery, The University of Tokyo Hospital, Tokyo, Japan
5 Department of Gastroenterology, Graduate School of Medicine, Juntendo University, Tokyo, Japan

Keywords
Pancreatobiliary (ERCP/PTCD), Strictures, ERC topics

received 12.12.2023
accepted after revision 25.3.2024
accepted manuscript online 2.4.2024

Bibliography
Endosc Int Open 2024; 12: E772–E780
DOI 10.1055/a-2298-0147
ISSN 2364-3722

Georg Thieme Verlag KG, Rüdigerstraße 14, 70469 Stuttgart, Germany

Corresponding author
Dr. Tsuyoshi Hamada, The University of Tokyo, Department of Gastroenterology, 7-3-1 Hongo, Bunkyo City, Tokyo 113-8655, Japan
hamada-tky@umin.ac.jp

Supplementary Material is available at https://doi.org/10.1055/a-2298-0147

ABSTRACT

Background and study aims Pancreatitis is a potentially lethal adverse event of endoscopic transpapillary placement of a self-expandable metal stent (SEMS) for malignant biliary obstruction (MBO). Deep learning-based image recognition has not been investigated in predicting pancreatitis in this setting.

Patients and methods We included 70 patients who underwent endoscopic placement of a SEMS for nonresectable distal MBO. We constructed a convolutional neural network (CNN) model for pancreatitis prediction using a series of pre-procedure computed tomography images covering the whole pancreas (≥ 120,960 augmented images in total). We examined the additional effects of the CNN-based probabilities on the following machine learning models based on clinical parameters: logistic regression, support vector machine with a linear or RBF kernel, random forest classifier, and gradient boosting classifier. Model performance was assessed based on the area under the curve (AUC) in the receiver operating characteristic analysis, positive predictive value (PPV), accuracy, and specificity.

Results The CNN model was associated with moderate levels of performance metrics: AUC, 0.67; PPV, 0.45; accuracy, 0.66; and specificity, 0.63. When added to the machine learning models, the CNN-based probabilities increased the performance metrics. The logistic regression model with the CNN-based probabilities had an AUC of 0.74, PPV of 0.85, accuracy of 0.83, and specificity of 0.96, compared with 0.72, 0.78, 0.77, and 0.96, respectively, without the probabilities.

Conclusions The CNN-based model may increase predictability for pancreatitis following endoscopic placement of a biliary SEMS. Our findings support the potential of deep learning technology to improve prognostic models in pancreatobiliary therapeutic endoscopy.

Introduction

In parallel with recent advances in high-performance computing technologies, machine learning algorithms have opened opportunities for reliable predictions of clinical outcomes of diseases by modeling linear and nonlinear contributions of and interactions between multiple parameters. Convolutional neural network (CNN)-based image recognition has emerged as a platform of artificial intelligence, which is increasingly utilized as a means of extracting abstract data from a series of medical images in an unbiased fashion [1, 2, 3, 4, 5]. In the field of diagnostic endoscopy for pancreatobiliary diseases, emerging evidence suggests the potential for a computer-assisted diagnosis system based on the CNN platform for endoscopic ultrasound (EUS) images to accurately identify incidental pancreatic cancer [6] or intraductal papillary mucinous neoplasm-derived carcinoma [7]. However, the utility of machine learning algorithms including CNN-based technologies has not been explored in clinical research on interventional endoscopy for pancreatobiliary diseases.

Endoscopic transpapillary deployment of a self-expandable metal stent (SEMS) has been the mainstay of nonsurgical palliative management of distal malignant biliary obstructions (MBOs) [8, 9, 10], given a longer functional time compared with plastic stents [11]. Pancreatitis has been a common adverse event (AE) of this procedure with potentially fatal outcomes [12, 13]. Therefore, a substantial number of studies have investigated risk factors for this AE, including stent mechanical properties, non-pancreatic cancer tumors, and contrast injection to the pancreatic duct during endoscopic retrograde cholangiopancreatography (ERCP) [14, 15, 16, 17]. Given evidence linking baseline morphological features of the pancreas to risk of pancreatitis following endoscopic SEMS placement [18], it is considered that there are ample opportunities for imaging information to facilitate risk prediction. However, the utility of deep learning algorithms (e. g., CNN) for pre-procedure cross-sectional images has not been investigated in this context.

To better predict risk of pancreatitis following endoscopic SEMS placement for nonresectable distal MBO, we developed machine learning-based models using not only clinical parameters but also the probabilities predicted via the CNN model using pre-procedure computed tomography (CT) images. We assessed the predictabilities of the models and examined the potential of CNN-based metrics to increase model performance for prediction of post-ERCP pancreatitis.

Patients and methods

Study design

The current study aimed to construct a CT-based CNN model to predict post-ERCP pancreatitis following endoscopic SEMS placement for nonresectable distal MBO and evaluated the additive effect of the CNN-based probabilities on the machine learning models based on clinical parameters (▶ **Fig. 1a**). We compared the models using the performance metrics including area under the curve (AUC) in the receiver operating characteristic (ROC) analysis, positive predictive value (PPV), accuracy, and specificity. Given the pilot nature of this feasibility study based on pancreatic morphology, we analyzed a single type of SEMS placed for nonresectable distal MBO (WallFlex; Boston Scientific, Massachusetts, United States) to exclude the possibility of differential pancreatitis risks by stent mechanical properties [17, 19]. This SEMS was one of the widely used SEMSs worldwide during the study period, and its properties and clinical outcomes were well documented [20, 21, 22].

Informed consent for research use of the data was obtained from all participants on an opt-out basis given the retrospective nature of the study. This study was designed and conducted according to the guidelines in the Helsinki Declaration (the latest version updated in 2013). The study was approved by the Ethics Committee at The University of Tokyo (Tokyo, Japan; approval number, #2058).

Study population

We screened consecutive patients who received initial SEMS placement for nonresectable distal MBO at The University of Tokyo Hospital (Tokyo, Japan) between March 2009 and March 2021 (▶ **Fig. 2**). We only included cases with available stent-naïve CT images. We excluded patients with a history of biliary SEMS placement and patients without available CT images. Distal MBO was defined as a malignant biliary stricture located ≥ 2 cm from communication of the bilateral hepatic ducts. All SEMS placement procedures were conducted on an inpatient basis, and the patients were followed every 2 to 4 weeks after discharge on an outpatient basis and through telephone interviews by study physicians until death or June 30, 2023, whichever came first.

Assessment of post-ERCP pancreatitis

The primary study endpoint was post-ERCP pancreatitis following biliary SEMS placement, which was defined as follows: 1) new or worsened abdominal pain; 2) prolonged hospitalization for at least 2 days; and 3) an elevated level of serum amylase (above three times the upper limit of normal), measured > 24 hours after ERCP [23, 24]. We routinely evaluated serum levels of amylase and pancreatic amylase 3 hours after ERCP and the following day. When pancreatitis was suspected based on clinical symptoms (e. g., abdominal pain, nausea) or blood tests, abdominal CT was conducted. We included pancreatitis events occurring within 14 days of the index ERCP procedure. Pancreatitis severity was graded according to the American Society of Gastrointestinal Endoscopy lexicon guidelines [25].

Endoscopic procedures

SEMSs were deployed via ERCP in a standard manner [26]. Cholangiography along with intraductal ultrasonography was performed to assess the status of biliary stricture and confirm the absence of accessory bile ducts. Sphincterotomy was carried out at the discretion of the endoscopist [27]. SEMSs were placed with the distal end being 5 to 10 mm in the duodenum. Prophylactic nonsteroidal anti-inflammatory drugs were not used routinely because the medications had not been approved for this indication during the study period in Japan. A prophy-

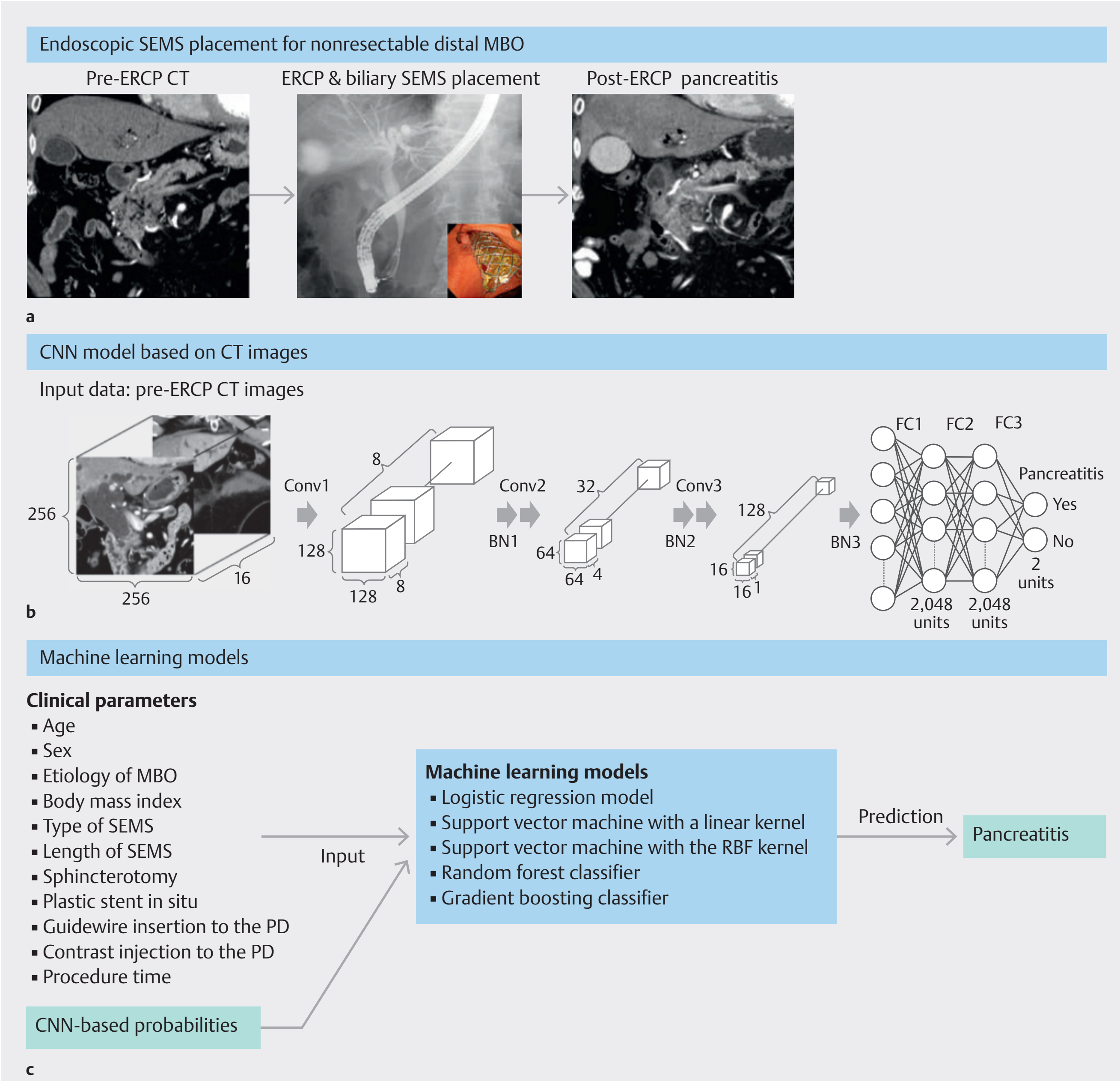

▶ **Fig. 1** Schematic overview of the current study. **a** Clinical scenario of endoscopic placement of a SEMS for nonresectable distal MBO. **b** Simplified structure of the CNN model. The CNN model based on pre-procedure CT images was constructed to calculate the predicted probabilities for post-ERCP pancreatitis. **c** Machine learning models for the prediction of post-ERCP pancreatitis. BN, batch normalization; CNN, convolutional neural network; Conv, convolutional layer; CT, computed tomography; ERCP, endoscopic retrograde cholangiopancreatography; FC, fully connected layer; MBO, malignant biliary obstruction; PD, pancreatic duct; RBF, radial basis function; SEMS, self-expandable metal stent.

lactic pancreatic duct stent was not placed in any of the patients. Procedure time was defined as the duration from the insertion to withdrawal of an endoscope.

CNN model based on pre-procedure CT images

The deep CNN model was constructed using a series of pre-procedure CT images of the pancreas as input data (the model structure is summarized in ▶ **Fig. 1b**). The study population (n = 70) was randomly split into five groups (n = 14 each) with the number of pancreatitis cases balanced between the groups. We trained the CNN model in a combined cohort of four groups and computed predictive probabilities of post-ERCP pancreatitis for each case in the remaining group. This procedure was repeated using each of the five groups as a validation set. A study radiologist (K.Y.) blinded to other clinical data conducted the image processing and model construction. The CNN models were constructed using Python (version, 3.8; Python Software Foundation, Wilmington, Delaware, United States) and the Chainer library. Image processing (i.e., cropping and augmentation) was performed using the Pillow library.

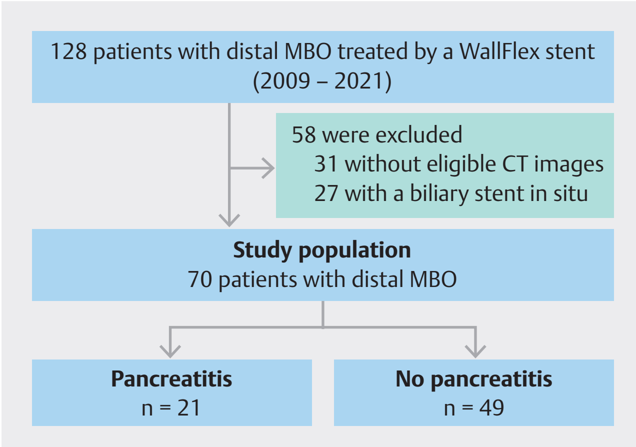

▶ **Fig. 2** Flow diagram of selection of patients receiving endoscopic placement of a biliary metal stent for nonresectable distal malignant biliary obstruction. CT, computed tomography; MBO, malignant biliary obstruction.

Contrast-enhanced (late arterial-phase) coronal-plane CT images (384 × 384 pixels) were extracted in the DICOM (Digital Imaging and Communications in Medicine) format. For each case, a consecutive series of 16 images (2 mm thick) covering the pancreas were selected, and 256 × 256 pixels well delineating the pancreatic parenchyma with the pancreatic duct were cropped from each image. Therefore, the shape of the input data for the CNN model was 256 × 256 × 16 pixels. The CNN model consisted of three convolutional layers and three batch normalizations, followed by three fully connected layers. The number of kernels for the convolutional layers were 8, 32, and 128. At each convolutional layer, 3 × 3-pixel kernels were convolved with a slide of two pixels for the first two convolutional layers and four pixels for the last convolutional layer, and the zero-padding. The number of units for the fully connected layers were 2,048, 2,048, and 2. Other hyperparameters used in the CNN model were as follows: optimizer, AdaGrad; error function, softmax cross entropy; batch size, 20; and the number of epochs, 20. The image data in the training process were augmented: i. e., parallel-shifted, rotated, flipped, contrast-changed, or brightness-changed images were generated for each original image (≥ 1,728 augmented images per case and ≥ 120,960 images in total).

Statistical analyses including other machine learning models

We utilized five machine learning algorithms that have been extensively validated and widely used for prediction of clinical outcomes of diseases [28, 29]: i. e., the logistic regression model, support vector machine (SVM) with a linear or radial basis function (RBF) kernel, random forest classifier, and gradient boosting classifier (▶ **Fig. 1c**). For the logistic regression model and SVM with a linear kernel, continuous variables were standardized. We assessed the importance of variables in a random forest classifier including the following variables: age (continuous), sex (male vs. female), etiology of MBO (pancreatic cancer vs. bile duct cancer vs. lymph node metastasis), body mass index (BMI, continuous), SEMS type (fully covered vs. partially covered vs. uncovered), SEMS length (continuous), endoscopic sphincterotomy (not performed vs. performed during a previous session vs. performed during the index session), a plastic stent in situ (absent vs. present), number of guidewire insertions to the pancreatic duct (continuous), contrast injection to the pancreatic duct (absent vs. present), and procedure time (continuous) as well as CNN-based probabilities. In addition to the CNN-based probabilities, we selected four variables with the highest feature importance for the final models: i. e., BMI, procedure time, age, and MBO etiology (**Supplementary Fig. 1**). We confirmed that inclusion of the whole set of covariates did not improve model performance (data not shown). Hyperparameters were determined using the grid search with 5-fold cross-validation (**Supplementary Table 1**). With a leave-one-out cross-validation, we computed the predicted probability of post-ERCP pancreatitis for each case in all models. Using the optimal threshold of probability determined based on the Youden index, we calculated performance metrics for the models. In secondary analyses, we assessed model performance stratified by BMI levels (which exhibited the highest feature importance) or other relevant parameters. All machine learning analyses were conducted using Python 3.11 and the Scikit-learn and xgboost libraries.

To compare clinical characteristics between patients with and without post-ERCP pancreatitis, we used Student's *t*-test for continuous variables and the chi-square or Fisher's exact test, as appropriate, for categorical variables. Two-sided $P < 0.05$ was considered statistically significant. Given multiple comparisons, the results were interpreted cautiously. These statistical analyses were conducted using SAS software (version 9.4; SAS Institute, Cary, North Carolina, United States).

Results

Among 70 patients with available coronal-plane images of pre-procedure CT, 21 patients (30%) developed post-ERCP pancreatitis with mild, moderate, and severe grades in 14, six, and one patient(s), respectively (▶ **Fig. 2**). **Supplementary Table 2** summarizes treatment and outcomes of patients with moderate- or severe-grade pancreatitis. Compared with patients with no pancreatitis, patients with pancreatitis were more likely to have higher BMI and non-pancreatic cancer as an etiology of distal MBO (▶ **Table 1**).

In an analysis of the CNN-based probabilities, PPV, accuracy, and specificity were 0.45, 0.66, and 0.71, respectively (▶ **Table 2**). In the ROC analysis, the CNN-based probabilities yielded an AUC of 0.67. When integrated into machine learning models, the CNN-based probabilities were associated with higher model performance (▶ **Table 2**). Taking an example of the logistic regression model yielding the largest AUC value based only on clinical parameters, the addition of the CNN-based probabilities was associated with increases in AUC (0.72 to 0.74), PPV (0.78 to 0.85), and accuracy (0.77 to 0.83). However, the addition resulted in no increase in specificity. The ROC curves are illustrated in **Supplementary Fig. 2**. In contrast, the addition of

▶ **Table 1** Demographic and procedure characteristics of patients receiving endoscopic placement of a biliary metal stent for nonresectable distal malignant biliary obstruction, overall or by the presence of post-procedure pancreatitis.

Characteristic*	All cases (n = 70)	Post-ERCP pancreatitis Absent (n = 49)	Post-ERCP pancreatitis Present (n = 21)	*P*
Demographics				
Mean age ± SD, years	68.1 ± 11.1	69.0 ± 10.7	66.0 ± 11.8	0.30
Sex				0.53
▪ Male	36 (51%)	24 (49%)	12 (57%)	
▪ Female	34 (49%)	25 (51%)	9 (43%)	
Cause of biliary obstruction				0.011
▪ Pancreatic cancer	65 (93%)	48 (98%)	17 (81%)	
▪ Bile duct cancer	3 (4.3%)	0	3 (14%)	
▪ Lymph node metastasis	2 (2.9%)	1 (2.0%)	1 (4.8%)	
Mean body mass index ± SD, kg/m^2	21.5 ± 3.4	20.9 ± 2.9	23.0 ± 3.9	0.015
Procedure characteristics				
Type of SEMS				0.61
▪ Fully covered	47 (67%)	31 (63%)	16 (76%)	
▪ Partially covered	21 (30%)	16 (33%)	5 (24%)	
▪ Uncovered	2 (2.9%)	2 (4.1%)	0	
Length of SEMS				0.15
▪ 40 mm	4 (5.7%)	1 (2.0%)	3 (14%)	
▪ 60 mm	35 (50%)	26 (53%)	9 (43%)	
▪ 80 mm	31 (44%)	22 (45%)	9 (43%)	
Diameter of SEMS				
▪ 10 mm	70 (100%)	49 (100%)	21 (100%)	NA
Endoscopic sphincterotomy				0.82
▪ No	10 (14%)	7 (14%)	3 (14%)	
▪ Yes (during a previous session)	23 (33%)	15 (31%)	8 (38%)	
▪ Yes (during the index session)	37 (53%)	27 (55%)	10 (48%)	
Plastic stent in situ				0.79
▪ Absent	35 (50%)	25 (51%)	10 (48%)	
▪ Present	35 (50%)	24 (49%)	11 (52%)	
Guidewire insertion to the PD				0.21
▪ None	48 (69%)	36 (73%)	12 (57%)	
▪ 1–5 times	17 (24%)	11 (22%)	6 (29%)	
▪ 6–10 times	5 (7.1%)	2 (4.1%)	3 (14%)	
PD injection				0.16
▪ Absent	58 (83%)	43 (88%)	15 (71%)	
▪ Present	12 (17%)	6 (12%)	6 (29%)	
Median procedure time (IQR), minutes	33 (20–53)	35 (25–50)	26 (18–57)	0.61

▶ **Table 1** (Continuation)

Characteristic[*]	**All cases (n = 70)**	**Post-ERCP pancreatitis**		***P***
		Absent (n = 49)	**Present (n = 21)**	
Prophylactic rectal diclofenac				0.30
▪ Absent	69 (99%)	49 (100%)	20 (95%)	
▪ Present	1 (1.4%)	0	1 (4.8%)	

[*]Percentage indicates the proportion of cases with a specific characteristic in all cases or each stratum of post-ERCP pancreatitis. Total percentages may not equal 100% due to rounding.
ERCP, endoscopic retrograde cholangiopancreatography; IQR, interquartile range; NA, not available; PD, pancreatic duct; SD, standard deviation; SEMS, self-expandable metal stent.

▶ **Table 2** Performance metrics of the models for prediction of pancreatitis following endoscopic placement of a biliary metal stent, with or without convolutional neural network (CNN)-based probabilities.

Model	**Performance metric**			
	AUC[*]	**PPV**	**Accuracy**	**Specificity**
CNN-based probabilities	0.67	0.45	0.66	0.63
Model without CNN-based probabilities				
▪ Logistic regression model	0.72	0.78	0.77	0.96
▪ Support vector machine (linear kernel)	0.72	0.78	0.77	0.96
▪ Support vector machine (RBF kernel)	0.59	1.00	0.79	1.00
▪ Random forest classifier	0.64	0.55	0.73	0.82
▪ Gradient boosting classifier	0.68	0.53	0.71	0.84
Model with CNN-based probabilities				
▪ Logistic regression model	0.74	0.85	0.83	0.96
▪ Support vector machine (linear kernel)	0.71	0.82	0.80	0.96
▪ Support vector machine (RBF kernel)	0.59	1.00	0.79	1.00
▪ Random forest classifier	0.65	0.53	0.71	0.84
▪ Gradient boosting classifier	0.67	0.56	0.73	0.84

[*]The AUC values were calculated using the receiver operating characteristic analysis.
AUC, area under the curve; CNN, convolutional neural network; PPV, positive predictive value; RBF, radial basis function.

the CNN-based probabilities was not associated with higher performance of the other machine learning models for prediction of post-ERCP pancreatitis (▶ **Table 2**).

We conducted secondary analyses stratified by the parameters that might affect risk of post-ERCP pancreatitis. Compared with patients with lower BMI, patients with higher BMI were more likely to experience post-ERCP pancreatitis (40% vs. 20%, respectively; $P = 0.068$). In an analysis stratified by BMI levels (▶ **Table 3**), the logistic regression model was associated with the highest AUC in the ROC analysis in both strata (0.70 and 0.68 for low and high levels of BMI, respectively). In the logistic regression model, all performance metrics examined were higher in the BMI-low group than in the BMI-high group. In an analysis stratified by age (**Supplementary Table 3**) or presence of a plastic stent in situ (**Supplementary Table 4**), the logistic regression model yielded the highest AUC in the ROC analysis in generally high-risk patients (i. e., younger patients and patients without a plastic stent) but not in low-risk patients. In addition, an analysis limited to covered SEMS yielded consistent results with the highest AUC in the ROC analysis in the logistic regression model (**Supplementary Table 5**).

▶ **Table 3** Performance metrics of the models with convolutional neural network-based probabilities for prediction of pancreatitis following endoscopic placement of a biliary metal stent, stratified by body mass index.

	Performance metric			
Model	**AUC***	**PPV**	**Accuracy**	**Specificity**
Body mass index, low (n = 35)†				
▪ Logistic regression	0.70	1.00	0.86	1.00
▪ Support vector machine (linear kernel)	0.59	0.67	0.83	0.96
▪ Support vector machine (RBF kernel)	0.13	1.00	0.86	1.00
▪ Random forest classifier	0.45	0	0.74	0.93
▪ Gradient boosting classifier	0.51	0	0.77	0.96
Body mass index, high (n = 35)†				
▪ Logistic regression	0.68	0.58	0.66	0.76
▪ Support vector machine (linear kernel)	0.62	0.55	0.63	0.76
▪ Support vector machine (RBF kernel)	0.31	0.80	0.69	0.95
▪ Random forest classifier	0.67	0.54	0.63	0.71
▪ Gradient boosting classifier	0.62	0.47	0.57	0.62

*The AUC values were calculated using the receiver operating characteristic analysis.
†Body mass index was dichotomized at the median value.
AUC, area under the curve; PPV, positive predictive value; RBF, radial basis function.

Discussion

In a consecutive series of patients with nonresectable distal MBO managed via endoscopic SEMS placement, the CNN-based profiling of pre-procedure CT images provided a modest predictive ability for post-ERCP pancreatitis. Adding the CNN-based probabilities to machine learning models resulted in increases in performance metrics (e. g., PPV and accuracy) without a decrease in specificity. The findings appeared to be robust in subpopulations classified by the most influential factor BMI. Our data support the potential for unbiased information extraction via the deep learning algorithm in facilitating prediction of post-ERCP pancreatitis in this patient population.

Utilizing pre-procedure CT images of pancreatic morphology under the deep CNN framework, we attempted to better predict risk of post-ERCP pancreatitis associated with endoscopic SEMS placement for distal MBO. In an investigation using pre-procedure CT images [18], estimated volume of the pancreatic parenchyma was well correlated with risk of post-ERCP pancreatitis in this setting. Using axial-plane CT images, the researchers manually measured the thickness of the pancreatic parenchyma (excluding the main pancreatic duct) at three prespecified pancreatic regions and found a positive association of the sum of the thickness values with pancreatitis risk. Despite its simplicity, this approach was limited by bias due to the nonautomated and thus operator-dependent measurement. The CNN captures the morphological information about the pancreatic ductal system, parenchymal texture, and pancreatic nodularity in a comprehensive unbiased fashion. Contrast-enhanced CT is routinely examined before biliary SEMS placement to evaluate the location and resectability of MBO and exclude the possibility of an accessory hepatic duct, and therefore, data on CT images are readily available in clinical practice. Therefore, predictive models via a deep learning approach for CT images may characterize risk of post-ERCP pancreatitis at no additional material cost in contrast to biomarker-based prediction approaches. Our data suggest that CNN-based probabilities per se may only provide a modest predictive ability for post-ERCP pancreatitis. However, in some of the widely utilized machine learning models, CNN-based probabilities contributed to reasonable model performance, working synergistically with relevant clinical parameters. Taken together, there may be ample opportunities for CNN-based pattern recognition to facilitate our prediction of post-ERCP pancreatitis.

Post-ERCP pancreatitis has been associated with substantial morbidity and mortality among patients receiving endoscopic biliary interventions [12, 13]; therefore, a large number of studies have investigated clinical parameters as potential risk factors as well as preventive measures for this procedure-related AE [30]. Risk stratification based on factors related to patients, procedures, and operators would help personalize peri-procedure care for patients receiving the treatment. Preventive measures (e. g., prophylactic pancreatic stent, nonsteroidal anti-inflammatory drugs, and hydration [31]) can be undertaken for patients who are predicted to be at high risk of developing post-ERCP pancreatitis. In randomized controlled trials of patients with nonresectable distal MBO [32, 33], researchers have demonstrated the feasibility of EUS-guided choledochoduodenostomy using a lumen-apposing metal stent with a higher technical success rate and comparable stent patency compared with ERCP-based SEMS placement. During EUS-guided drainage, the mechanical burden on the pancreatic ductal system and resultant pancreatic inflammation may be minimized. Given the risks of specific AEs associated with EUS-guided drainage (e. g., bile leak), further research is warranted to determine the most appropriate drainage strategy for patients with distal MBO overall. Nonetheless, EUS-guided drainage may be a reasonable alternative to endoscopic transpapillary drainage in patients who are predicted to be at high risk of post-ERCP pancreatitis based on the CNN-based pipeline. Further research is warranted to optimize drainage strategies for distal MBO according to the CNN-based risk prediction for post-ERCP pancreatitis. A much larger number of patients receive ERCP for various indications, and prevention of post-ERCP pancreatitis in this population may have a substantial impact on burdens to patients and the health care system. Therefore, the utility of CNN-based stratification of risk of post-ERCP pancreatitis should be investigated in patients receiving ERCP overall. In addition, scoring systems based on different sets of clinical parameters from the current study have been reported for prediction of post-ERCP pancreatitis [34, 35]. Therefore, future research is warranted to investigate whether integration of deep learning-based image recognition with these scoring systems improves predictive ability.

We acknowledge the potential limitations of the current investigation. First, we analyzed a single type of SEMS with the same diameter. This inclusion criterion excluded the influence of differential risks of post-ERCP pancreatitis associated with mechanical properties of the SEMSs [17, 19] while allowing us to focus on clinical parameters and morphological signatures of the pancreas in risk stratification of post-ERCP pancreatitis. Nonetheless, external validation including various types of SEMSs is required to ensure the generalizability of our conclusions. Second, despite our extensive efforts in data augmentation during construction of the CNN model, the small sample size of the total study population might limit the robustness of our findings. In the machine learning models (e. g., SVM), the small sample size of cases and events compared with the number of variables might result in model overfitting, thereby reducing the predictive abilities in the validation sets. Therefore, further investigation of the machine learning models using multicenter data with an external test set is desirable.

Conclusions

In conclusion, the deep CNN model based on pre-procedure CT images appeared to synergize with clinical parameters in risk stratification for pancreatitis following endoscopic SEMS placement for nonresectable distal MBO. There may be opportunities for the deep learning platform to contribute to refinement of prognostic models in therapeutic endoscopy for pancreatobiliary diseases.

Acknowledgement

T.H. and K.Y. contributed equally as co-first authors.

Conflict of Interest

Y.N. and H.I. receive research funding and honoraria from Boston Scientific Japan. This work was not funded by this company. No other conflicts of interest exist. The other authors declare that they have no conflicts of interest.

References

[1] Pan Y, He L, Chen W et al. The current state of artificial intelligence in endoscopic diagnosis of early esophageal squamous cell carcinoma. Front Oncol 2023; 13: 1198941 doi:10.3389/fonc.2023.1198941

[2] Jahagirdar V, Bapaye J, Chandan S et al. Diagnostic accuracy of convolutional neural network-based machine learning algorithms in endoscopic severity prediction of ulcerative colitis: a systematic review and meta-analysis. Gastrointest Endosc 2023; 98: 145–154.e148

[3] Sharma P, Hassan C. Artificial intelligence and deep learning for upper gastrointestinal neoplasia. Gastroenterology 2022; 162: 1056–1066 doi:10.1053/j.gastro.2021.11.040

[4] Xie X, Xiao YF, Zhao XY et al. Development and validation of an artificial intelligence model for small bowel capsule endoscopy video review. JAMA Netw Open 2022; 5: e2221992 doi:10.1001/jamanetworkopen.2022.21992

[5] Tonozuka R, Mukai S, Itoi T. The role of artificial intelligence in endoscopic ultrasound for pancreatic disorders. Diagnostics (Basel, Switzerland) 2020; 11: 18

[6] Tonozuka R, Itoi T, Nagata N et al. Deep learning analysis for the detection of pancreatic cancer on endosonographic images: a pilot study. J Hepatobiliary Pancreat 2021; 28: 95–104 doi:10.1002/jhbp.825

[7] Kuwahara T, Hara K, Mizuno N et al. Usefulness of deep learning analysis for the diagnosis of malignancy in intraductal papillary mucinous neoplasms of the pancreas. Clin Transl Gastroenterol 2019; 10: 1–8 doi:10.14309/ctg.0000000000000045

[8] Eisenberg I, Gaidhane M, Kahaleh M et al. Drainage approach for malignant biliary obstruction: a changing paradigm. J Clin Gastroenterol 2023; 57: 546–552 doi:10.1097/MCG.0000000000001854

[9] Nakai Y, Isayama H, Wang HP et al. International consensus statements for endoscopic management of distal biliary stricture. J Gastroenterol Hepatol 2020; 35: 967–979 doi:10.1111/jgh.14955

[10] Bill JG, Mullady DK. Stenting for benign and malignant biliary strictures. Gastrointest Endosc Clin N Am 2019; 29: 215–235 doi:10.1016/j.giec.2018.12.001

[11] Almadi MA, Barkun A, Martel M. Plastic vs. self-expandable metal stents for palliation in malignant biliary obstruction: a series of meta-analyses. Am J Gastroenterol 2017; 112: 260–273 doi:10.1038/ajg.2016.512

[12] Buxbaum JL, Freeman M, Amateau SK et al. American Society for Gastrointestinal Endoscopy guideline on post-ERCP pancreatitis prevention strategies: summary and recommendations. Gastrointest Endosc 2023; 97: 153–162 doi:10.1016/j.gie.2022.10.005

[13] Dumonceau JM, Kapral C, Aabakken L et al. ERCP-related adverse events: European Society of Gastrointestinal Endoscopy (ESGE) Guideline. Endoscopy 2020; 52: 127–149 doi:10.1055/a-1075-4080

[14] Tamura T, Yamai T, Uza N et al. Adverse events of self-expandable metal stent placement for malignant distal biliary obstruction: a large multicenter study. Gastrointest Endosc 2024; 99: 61–72.e68

[15] Kim GH, Ryoo SK, Park JK et al. Risk factors for pancreatitis and cholecystitis after endoscopic biliary stenting in patients with malignant extrahepatic bile duct obstruction. Clin Endosc 2019; 52: 598–605

[16] Shimizu S, Naitoh I, Nakazawa T et al. Predictive factors for pancreatitis and cholecystitis in endoscopic covered metal stenting for distal malignant biliary obstruction. J Gastroenterol Hepatol 2013; 28: 68–72 doi:10.1111/j.1440-1746.2012.07283.x

[17] Kawakubo K, Isayama H, Nakai Y et al. Risk factors for pancreatitis following transpapillary self-expandable metal stent placement. Surg Endosc 2012; 26: 771–776 doi:10.1007/s00464-011-1950-4

[18] Takeda T, Sasaki T, Mie T et al. Novel risk factors for recurrent biliary obstruction and pancreatitis after metallic stent placement in pancreatic cancer. Endosc Int Open 2020; 8: E1603–E1610 doi:10.1055/a-1244-1989

[19] Isayama H, Nakai Y, Toyokawa Y et al. Measurement of radial and axial forces of biliary self-expandable metallic stents. Gastrointest Endosc 2009; 70: 37–44 doi:10.1016/j.gie.2008.09.032

[20] Kogure H, Ryozawa S, Maetani I et al. A prospective multicenter study of a fully covered metal stent in patients with distal malignant biliary obstruction: WATCH-2 Study. Digest Dis Sci 2018; 63: 2466–2473

[21] Yokota Y, Fukasawa M, Takano S et al. Partially covered metal stents have longer patency than uncovered and fully covered metal stents in the management of distal malignant biliary obstruction: a retrospective study. BMC Gastroenterol 2017; 17: 105

[22] Isayama H, Mukai T, Itoi T et al. Comparison of partially covered nitinol stents with partially covered stainless stents as a historical control in a multicenter study of distal malignant biliary obstruction: the WATCH study. Gastrointest Endosc 2012; 76: 84–92

[23] Cotton PB, Lehman G, Vennes J et al. Endoscopic sphincterotomy complications and their management: an attempt at consensus. Gastrointest Endosc 1991; 37: 383–393

[24] Isayama H, Hamada T, Yasuda I et al. TOKYO criteria 2014 for transpapillary biliary stenting. Dig Endosc 2015; 27: 259–264 doi:10.1111/den.12379

[25] Cotton PB, Eisen GM, Aabakken L et al. A lexicon for endoscopic adverse events: report of an ASGE workshop. Gastrointest Endosc 2010; 71: 446–454 doi:10.1016/j.gie.2009.10.027

[26] Hamada T, Isayama H, Nakai Y et al. Tips and troubleshooting for transpapillary metal stenting for distal malignant biliary obstruction. J Hepatobiliary Pancreat 2014; 21: E12–18 doi:10.1002/jhbp.51

[27] Kato S, Kuwatani M, Onodera M et al. Risk of pancreatitis following biliary stenting with/without endoscopic sphincterotomy: a randomized controlled trial. Clin Gastroenterol Hepatol 2022; 20: 1394–1403.e1391

[28] Silva GFS, Fagundes TP, Teixeira BC et al. Machine learning for hypertension prediction: a systematic review. Curr Hypertension Rep 2022; 24: 523–533 doi:10.1007/s11906-022-01212-6

[29] Spann A, Yasodhara A, Kang J et al. Applying machine learning in liver disease and transplantation: a comprehensive review. Hepatology 2020; 71: 1093–1105 doi:10.1002/hep.31103

[30] Wu CCH, Lim SJM, Khor CJL. Endoscopic retrograde cholangiopancreatography-related complications: risk stratification, prevention, and management. Clin Endosc 2023; 56: 433–445 doi:10.5946/ce.2023.013

[31] Akshintala VS, Sperna Weiland CJ, Bhullar FA et al. Non-steroidal anti-inflammatory drugs, intravenous fluids, pancreatic stents, or their combinations for the prevention of post-endoscopic retrograde cholangiopancreatography pancreatitis: a systematic review and network meta-analysis. Lancet Gastroenterol Hepatol 2021; 6: 733–742 doi:10.1016/S2468-1253(21)00170-9

[32] Chen YI, Sahai A, Donatelli G et al. Endoscopic ultrasound-guided biliary drainage of first intent with a lumen-apposing metal stent vs endoscopic retrograde cholangiopancreatography in malignant distal biliary obstruction: a multicenter randomized controlled study (ELEMENT trial). Gastroenterology 2023; 165: 1249–1261.e1245

[33] Teoh AYB, Napoleon B, Kunda R et al. EUS-guided choledocho-duodenostomy using lumen apposing stent versus ERCP with covered metallic stents in patients with unresectable malignant distal biliary obstruction: a multicenter randomized controlled trial (DRA-MBO Trial). Gastroenterology 2023; 165: 473–482.e472

[34] Fukuda R, Hakuta R, Nakai Y et al. Development and external validation of a nomogram for prediction of post-endoscopic retrograde cholangiopancreatography pancreatitis. Pancreatology 2023; 23: 789–796 doi:10.1016/j.pan.2023.08.008

[35] Fujita K, Yazumi S, Uza N et al. New practical scoring system to predict post-endoscopic retrograde cholangiopancreatography pancreatitis: Development and validation. JGH Open 2021; 5: 1078–1084 doi:10.1002/jgh3.12634